2016

Comparison on Evaporation Heat Transfer between R32/R1234yf and R32/R1234ze(E) Flowing in Horizontal Microfin Tubes

Shingo Nakamura
Kyushu university, Japan, 2es14187w@s.kyushu-u.ac.jp

Chieko Kondou
Nagasaki university, Japan, ckondou@nagasaki-u.ac.jp

Nobuo Takata
Kyushu university, Japan, purdueherrickconf16@gmail.com

Shigeru Koyama
Kyushu university, Japan, koyama@cm.kyushu-u.ac.jp

Comparison on Evaporation Heat Transfer between R32/R1234yf and R32/R1234ze(E) Flowing in Horizontal Microfin Tubes

Shingo NAKAMURA[1], Chieko KONDOU[2]*, Nobuo TAKATA[1], Shigeru KOYAMA[1, 3]

[1] Kyushu University, Interdisciplinary Graduate School of Engineering Science
Fukuoka, Japan

[2] Nagasaki University, Graduate School of Engineering
Nagasaki, Japan
(ckondou@nagasaki-u.ac.jp)

[3] Kyushu University, International Institute for Carbon-Neutral Energy Research
Fukuoka, Japan
(koyama@phase.cm.kyushu-u.ac.jp)

ABSTRACT

Refrigerant mixtures R32/R1234yf and R32/R1234ze(E) are considered to be the low GWP alternatives to R32 and R410A used in air conditioners. However, according to recent reports, severe heat transfer degradation occurs during the evaporation process. This implies that much larger heat exchangers are required to maintain the COP and cooling/heating capacity to adapt to R32/R1234yf and R32/R1234ze(E). The effects of the components and composition of the mixture on the heat transfer degradation are experimentally investigated in this study. The heat transfer coefficient of the two mixtures and their individual components, i.e., R32, R1234yf and R1234ze(E), are experimentally quantified using horizontal copper microfin tubes with 6.00-mm outer diameters and 48, 58, and 64 fins, with 0.26-mm heights and 19 ° helical angles. The evaporation test is conducted at an average saturation temperature of 10 °C, a heat flux of 10 kW m^{-2}, and mass fluxes from 150 to 400 kg $m^{-2}s^{-1}$.

1. INTRODUCTION

Refrigerants R1234yf and R1234ze(E) with GWP_{100} (global warming potential of 100-year time horizon) less than 1 (Myhre et al., 2013) have been proposed to replace R134a in automotive air-conditioners and also R410A in residential air-conditioning applications. However, results of some drop-in tests with 2.0-kW class air-conditioning units showed that the use of R1234yf or R1234ze(E) alone drastically decreases the heat load and COP (coefficient of performance) from that achieved with R410A. The primary cause of this decrease is attributed to the considerably smaller volumetric capacity of the new refrigerants. Therefore, to increase the volumetric capacity while preserving the low GWP, R32 is added to both R1234yf and R1234ze(E). Refrigerant mixtures with various amounts of the additive are proposed by the manufacturers and assigned new designations by ASHRAE (AHRAE, 2015). Unlike R410A, most of the newly assigned low-GWP mixtures are zeotropic. The performance improvements from the addition of R32 were experimentally confirmed using several air-conditioning units (Wang and Amrane, 2014); however, the necessity or limitation of optimizations for these new refrigerant mixtures remains many unclear points. Heat exchanger design is one area that has not been well-studied. As reported in the literature (Jung and Radermacher, 1993; Wettermann and Steiner, 2000), the volatility difference present in these zeotropic mixtures results in severe degradation during flow boiling heat transfer. Therefore, larger heat exchangers are required to maintain cycle performance with the low-GWP refrigerant mixtures.

In this study, flow boiling heat transfer in R32/R1234yf and R32/R1234ze(E) in a horizontal microfin tube, with an outer diameter of 6.0 mm, is experimentally determined. The quantified heat transfer coefficients and pressure gradients of the two mixtures at various mass fractions are compared. The data show the influence of the temperature glide and volatility difference on the heat transfer.

2. EXPERIMENT

Figure 1 (a) illustrates the experimental loop used to characterize the flow boiling heat transfer of R32/R1234yf and R32/R1234ze(E). The refrigerant loop is a vapor compression heat pump cycle with heat source/sink water loops. The HTC (heat transfer coefficient) and pressure drop are measured in the test sections, which also functions as the evaporator. To determine the bulk enthalpies of superheated vapor, the bulk mean temperature and the pressure are measured in mixing chambers placed at the outlet of the superheater. The circulation composition of the mixture is measured by sampling approximately 1 cc of subcooled liquid at the outlet of the liquid reservoir. The sampled liquid is completely vaporized in the sampling vessel and then assayed using a thermal conductivity detector gas chromatograph. The refrigerant state is always evaluated at the circulation composition. Based on the bulk enthalpies of the superheated vapor, the enthalpies in the test sections are calculated using the enthalpy changes in the superheater obtained from the heat balance over the heat source water.

Figure 1 (b) shows two subsections of the test section to explain the structure. A horizontally oriented test microfin tube is surrounded by four water jackets, i.e., the subsections. Pressure ports are bored (0.6-mm ID) between the subsections to measure the heat transfer rates over the 414-mm length and the pressure drop at 554-mm intervals. At the center of each subsection, four thermocouples are embedded in the outside tube wall. The internal tube surface temperature, T_{wi}, is obtained by one-dimensional heat conduction through the tube wall as follows:

$$T_{wi} = \left(T_{wo,top} + T_{wo,bottom} + T_{wo,right} + T_{wo,left}\right)/4 + \left[Q_{H2O}/\left(2\pi\Delta Z\lambda_{tube}\right)\right]\ln\left(D_o/d_{eq}\right) \tag{1}$$

where Q_{H2O} is the heat transfer rate in a subsection considering the heat loss to the ambient through the insulators. The representative refrigerant temperature of each subsection, T_r, is defined as the arithmetic mean of the inlet and outlet, calculated from the enthalpies and pressures with REFPROP 9.1 (Lemmon et al., 2013), assuming thermodynamic equilibrium as follows:

$$T_r = \left(T_{r,in} + T_{r,out}\right)/2 \tag{2}$$

$$T_{r,in} = f_{equilibrium}\left(h_{in}, P_{in}, X_{R32}\right),\ T_{r,out} = f_{equilibrium}\left(h_{out}, P_{out}, X_{R32}\right) \tag{3, 4}$$

Similarly, the representative vapor quality of each subsection, x, is calculated as follows:

$$x = \left(x_{in} + x_{out}\right)/2 \tag{5}$$

$$x_{in} = f_{equilibrium}\left(h_{in}, P_{in}, X_{R32}\right),\ x_{out} = f_{equilibrium}\left(h_{out}, P_{out}, X_{R32}\right) \tag{6, 7}$$

where X_{R32} is the circulation composition of R32 determined by the liquid sampling.

Table 1 specifies the dimensions of the test microfin tube based on the symbols in the microscopic cross-sectional area of Figure 2. The equivalent inner diameter, d_{eq}, is the diameter of a smooth tube that envelops an equal free-flow volume. The surface enlargement, η_A, is the ratio of the actual heat transfer area to that of the equivalent smooth tube.

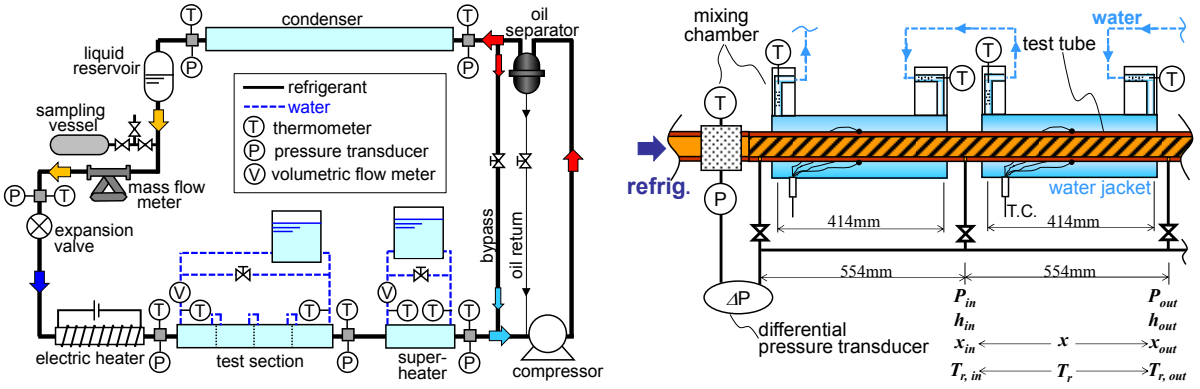

(a) test loop (b) test section (two subsections)

Figure 1: Experimental apparatus

Table 1 Dimensions of the test microfin tube

outer diameter	d_o	6.00	mm
fin tip diameter	d_{min}	4.80	mm
fin root diameter	d_{max}	5.32	mm
equivalent diameter	d_{eq}	5.26	mm
fin height	h_{fin}	0.256	mm
helix angle	β_{fin}	18.5	°
apex angle	γ_{fin}	15.4	°
number of fins	N_{fin}	64	-
surface enlargement base on a smoot tube	η_A	2.74	-

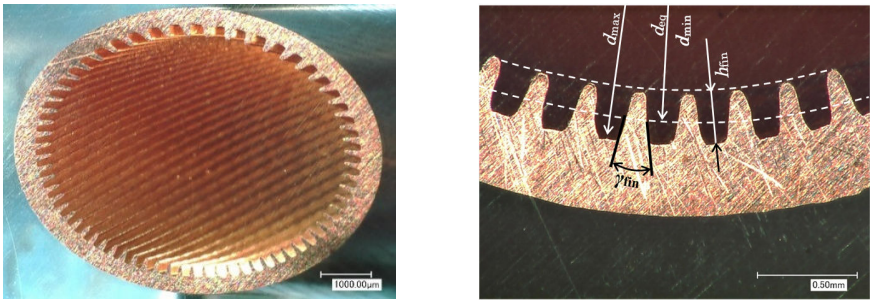

(a) 45 ° cut surface (b) cross-sectional microscopic picture

Figure 2: The test microfin tube

Table 2 Thermophysical properties of the test refrigerants at an average saturation temperature of 10 °C

		R32	R1234yf	R1234ze(E)	R32/R1234yf (0.5/0.5 mass%)	R32/R1234ze(E) (0.5/0.5 mass%)
pressure	P	1.11	0.44	0.31	0.77	0.80
temperature glide	ΔT_{glide}	0	0	0	5.46	7.36
latent heat	Δh_{LV}	299	157	178	236	238
liquid density	ρ_L	1020	1144	1210	[1] 1087	[1] 1096
vapor density	ρ_V	30.2	24.3	16.5	[2] 27.6	[2] 28.5
liquid viscosity	μ_L	135	185	238	155	160
liquid thermal conductivity	λ_L	0.137	0.068	0.079	0.105	0.108

[1] at a bubble point [2] at a dew point

Refrigerant mass flux is defined based on the average cross-sectional area of free-flow volume. Based on the actual heat transfer area, the heat flux q_{wi}, and the HTC α are as follows:

$$\alpha = q_{wi} / \left(T_r - T_{wi} \right), \quad q_{wi} = Q_{H2O} / \left(\pi d_{eq} \eta_A \Delta Z \right) \tag{8, 9}$$

A deviation of up to 1 kW m^{-2} of the targeted average heat flux is allowed to adjust for the test conditions, except for the dryout condition during evaporation. The measurements are conducted at the saturation temperature of 10 °C, which is the average of the bubble temperature and the dew temperature.

Table 2 lists the thermophysical properties of the test refrigerants at an average saturation temperature, $(T_{bub}+T_{dew})/2$, of 10 °C, as calculated with REFPROP 9.1 (Lemmon et al., 2013). The test mixtures are compared at a mass fraction of 50/50 mass%. The latent heat and thermal conductivity of R32 are approximately two times greater than those of R1234yf and R1234ze(E). This suggests that the boiling heat transfer performance of R32/R1234yf and R32/R1234ze(E) can be improved by adding R32. However, as found in previous studies (Celata et al., 1994; Stephan and Kern, 2004), the volatility difference represented by the temperature glide can compensate for the improvement in boiling heat transfer. The temperature glide of R32/R1234ze(E) is 1.9 K larger than that of R32/R1234yf at a mass fraction of (50/50 mass%).

3. RESULTS AND DISCUSSION

Figure 3 shows the experimentally obtained HTC for R32, R1234yf, and R1234ze(E) at an average saturation temperature of 10 °C and a heat flux of 10 kW m^{-2}. The horizontal and vertical bars on the symbols show the measurement uncertainties in HTC and vapor quality change over a subsection. The general trend in the HTC data is similar to that already reported in the literature (Diani et al., 2015). The exception is the high HTC that occurs at a vapor quality of approximately 0.8. Because of the small temperature difference between the refrigerant and the tube wall, the uncertainty in HTC becomes large at vapor qualities above 0.8, especially in the case of R32. Comparing the experimental HTC at vapor qualities from 0.2 to 0.6, R32 exhibits obviously higher HTC values than the other two refrigerants. While, R1234yf exhibits a slightly higher HTC than R1234ze(E), except for the case of a mass flux of 150 kg $m^{-2}s^{-1}$. At a mass flux of 150 kg $m^{-2}s^{-1}$, the HTC of R1234yf started decreasing at a vapor quality of 0.5.

Figure 4 shows the experimental values of HTC for R32/R1234yf and R32/R1234ze(E) at three different concentrations of R32 mass fraction. Except in the case of R32/R1234yf (69/31 mass%), the HTC of those the R32/R1234yf mixture is significantly lower than that of the single component, as shown in Figure 3. This significant heat transfer degradation is shown in the nucleate boiling dominant region of low vapor quality and also in the convective evaporation dominant region of high vapor quality. Of the zeotropic mixtures, the nucleate boiling suppression by volatility difference is investigated in previous studies (e.g., Thome, 1983). According to Kern and Stephan (2003), the capillary pressure influences the liquid-vapor equilibrium and the concentration gradient in a micro region around the nucleate bubbles, severely suppressing nucleate boiling. In addition, the concentration boundary layer on the vapor-liquid interface suppresses the convective evaporation, resulting in a reduction of the effective superheat from the temperature glide (Stephan, 1992). In summary, the contribution of nucleate boiling and convective boiling are both suppressed in zeotropic mixtures.

At a mass fraction of 28/72 mass%, R32/R1234yf and R32/R1234ze(E) exhibit similar heat transfer performance. The HTC of R32/R1234yf barely exceeds R32/R1234ze(E) at vapor qualities below 0.7. At a mass fraction of 45/55 mass%, the difference in HTC between R32/R1234yf and R32/R1234ze(E) is more evident. As the mass fraction of R32 increases from 28 to 45 mass%, the HTC of those two mixtures increases somewhat at vapor quality below 0.8. At a mass fraction of 69/31 mass%, the HTC of R32/R1234yf is different from that of R32/R1234ze(E). The HTC of R32/R1234yf is almost comparable to that of R32 alone. The mass transfer resistance that suppresses nucleate boiling and convective evaporation appears to be mitigated in R32/R1234yf flow boiling.

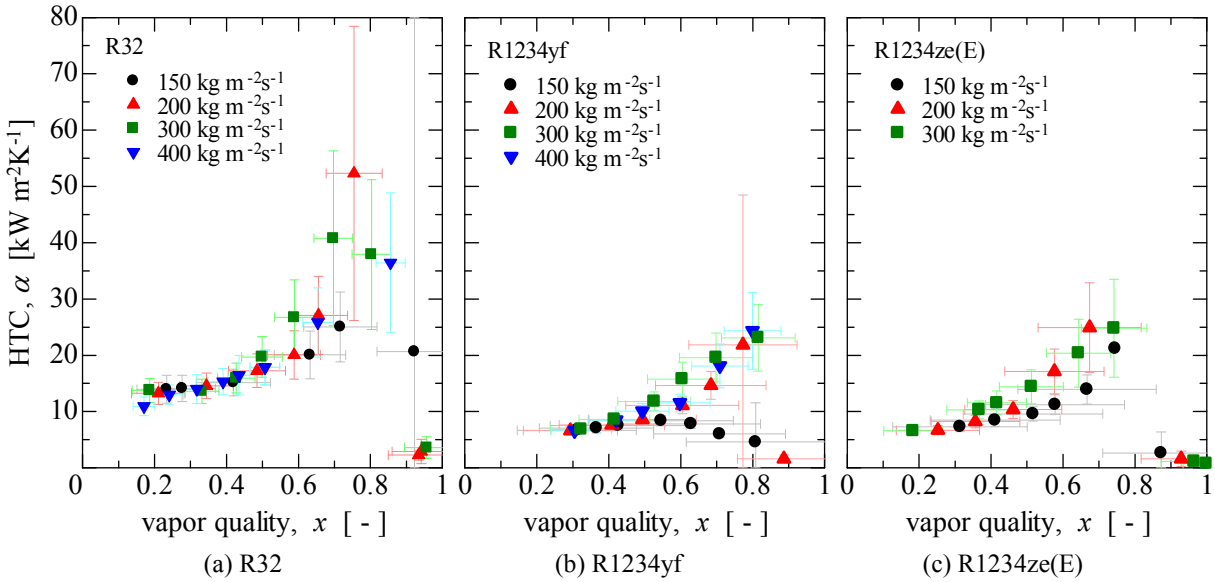

(a) R32 (b) R1234yf (c) R1234ze(E)

Figure 3: Experimental HTC of each component at 10 °C and 10 kWm^{-2}.

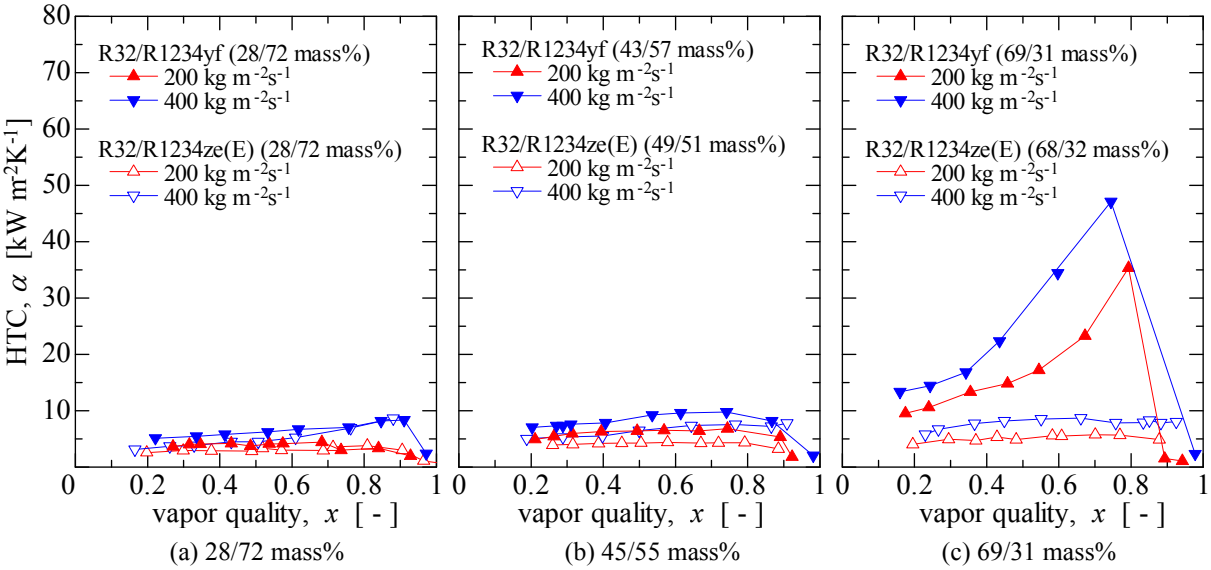

Figure 4: Experimental HTC of mixtures at varied mass fractions.

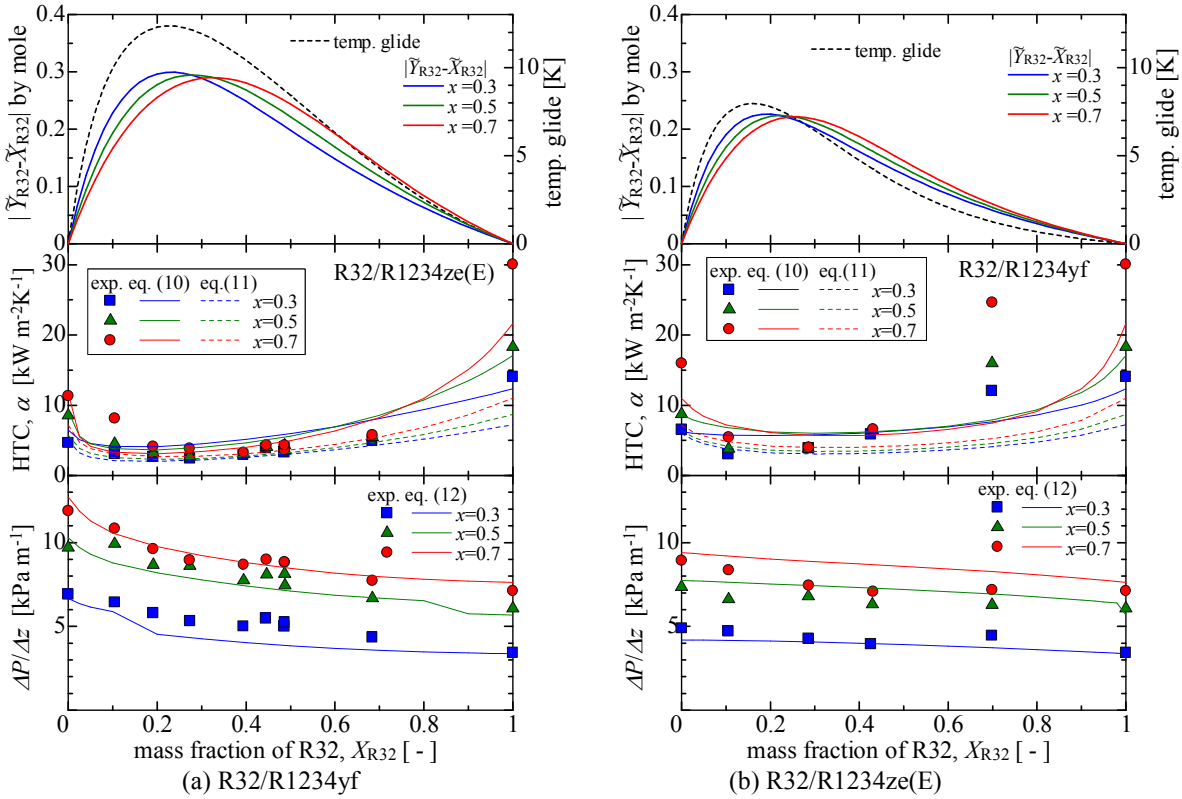

Figure 5: Variation in vapor-liquid equilibrium, HTC and pressure drop against the circulation mass fraction at 200 kgm^{-2}s^{-1} and 10 kWm^{-2}.

Figure 5 shows variations in the temperature glide, the mole fraction difference, the experimental HTC, and the experimental pressure drop as functions of the mass fraction of R32. The mass fractions of 0 and 1 mean R1234yf or R1234ze(E) alone and R32 alone, respectively. To show the variation, the experimental data are interpolated and compared at vapor qualities of 0.3, 0.5, and 0.7 for a mass flux of 200 kg m^{-2}s^{-1} and a heat flux of 10 kWm^{-2}. In the

Table 3 Summary of the predicting correlations plotted in Figure 5

Cavallini et al. (1983)

$$\alpha = \left(\frac{d_{\min}}{d_{\text{eq}}\eta_{\text{A}}}\right)\left[\frac{1}{\alpha_{\text{f}}} + xCp_{\text{V}}\frac{\Delta T_{\text{glide}}}{\left(h_{\text{dew}} - h_{\text{bub}}\right)}\frac{1}{\alpha_{\text{V}}}\right]^{-1} \tag{10}$$

where, $\alpha_{\text{f}} = \alpha_{\text{nb}}F_{\text{C}} + \alpha_{\text{LO}}F$, $\alpha_{\text{nb}} = \left[55P_{\text{R}}^{0.12}\left(-\log_{10}P_{\text{R}}\right)^{-0.55}M^{-0.5}q_{\text{en}}^{0.67}\right]\ SF_1$,

$F_{\text{C}} = \left\{1 + \left(\frac{\alpha_{\text{id}}\Delta T_{\text{glide}}}{q_{\text{wi}}}\right)\left[1 - \exp\left(-\frac{q_{\text{wi}}}{\rho_{\text{L}}\left(h_{\text{dew}} - h_{\text{bub}}\right)\beta_{\text{L}}}\right)\right]\right\}^{-1}$, $\alpha_{\text{id}} = \alpha_{\text{nb}} + \alpha_{\text{cv}}F$

$\alpha_{\text{cv}} = \left[\lambda_{\text{L}}/\left(0.01/d_{\min}\right)\right]Nu_{\text{cv,sm}}\,Rx^{2.14}\left(Bo\cdot Fr\right)^{A}\,F_2\,F_3$, $Nu_{\text{cv,sm}} = \left[0.023\left(\frac{Gd_{\min}}{\mu_{\text{L}}}\right)Pr_{\text{L}}^{1/3}\right]\left[\left(1-x\right) + 2.63\cdot x\left(\frac{\rho_{\text{L}}}{\rho_{\text{V}}}\right)^{0.5}\right]^{0.8}$

$S = 1.36X_{tt}^{\ 0.36}$, $F_1 = \left(\frac{0.01}{d_{\min}}\right)^{0.38}$, $q_{\text{en}} = \alpha_{\text{nb}}\left(T_{\text{wi}} - T_{\text{sat}}\right)$, $Bo = \frac{g\rho_{\text{L}}h_{\text{fin}}\pi d_{\min}}{8\sigma N_{\text{fin}}}$, $Fr = \frac{u_{\text{VO}}^2}{gd_{\min}}$, $Rx = \frac{\eta_{\text{A}}d_{\text{eq}}}{d_{\min}}$,

$F_2 = \left(\frac{0.01}{d_{\min}}\right)^{C_5}$, $F_3 = \left(\frac{100}{G_{r,\min}}\right)^{0.59}$, $C_5 = \begin{cases} -0.15\left(G < 500\ \text{kg m}^{-2}\text{s}^{-1}\right) \\ -0.21\left(G \geq 500\ \text{kg m}^{-2}\text{s}^{-1}\right) \end{cases}$, C_7= 0.36, $\beta_{\text{L}} = 0.0003$.

Kondou et al. (2013)

$$\alpha = \left[\frac{1}{\alpha_{\text{V}}}\left(xCp_{\text{V}}\left.\frac{dT_{\text{sat}}}{dh}\right|_{p}\right) + \frac{1 + C_{\text{ir}}\left(\tilde{Y}_1 - \tilde{X}_1\right)}{\left(\alpha_{\text{cv}} + \alpha_{\text{nb,mix}}\right)}\right]^{-1} \tag{11}$$

where, $\alpha_{\text{V}} = \left(\frac{\lambda_{\text{V}}}{d_{\text{eq}}}\right)0.023\left(\frac{G_{\text{r}}d_{\text{eq}}}{\mu_{\text{V}}}\right)^{0.8}Pr^{\frac{1}{3}}$, $\left.\frac{dT_{\text{sat}}}{dh}\right|_{p} \cong \frac{T_{\text{dew}} - T_{\text{bub}}}{\Delta h_{\text{LV}}}$, $\alpha_{\text{cv}} = \alpha_{\text{L\_Carnavos}}\left(1 + \frac{C_{\text{cv}}}{X_{tt}}\right)$,

$\alpha_{\text{L\_Carnavos}} = \frac{\lambda_{\text{L}}}{\left(d_{\text{eq}}/\eta_{\text{A}}\right)}0.023\left[\frac{G_{\text{r}}\left(1-x\right)\left(d_{\text{eq}}/\eta_{\text{A}}\right)}{\mu_{\text{L}}}\right]^{0.8}Pr^{0.4}\times\left[\left(\frac{d_{\text{eq}}}{d_{\max}}\right)^{0.2}\left(\frac{d_{\max}}{d_{\text{eq}}\eta_{\text{A}}}\right)^{0.5}\left(\frac{1}{\cos\beta}\right)^{3}\right]$

$C_{\text{cv}} = 10\left(Re_{\text{L}}\times 10^{-4}\right)^{-0.6}\left[1 - 0.93\exp\left(-4\cdot Re_{\text{L}}\times 10^{-4}\right)\right]\left(\rho_{\text{V}}/\rho_{\text{L}}\right)^{0.35}$, $\alpha_{\text{nb,mix}} = \left(\frac{\tilde{X}_1}{\alpha_{\text{nb},1}} + \frac{\tilde{X}_2}{\alpha_{\text{nb},2}}\right)^{-1} \times N_{\text{Sn}}^{\ \frac{7}{5}}$,

$N_{\text{Sn}} = \left[1 - \left(\tilde{Y}_1 - \tilde{X}_1\right)\left(\frac{a_{\text{L}}}{D_{12,\text{L}}}\right)^{1/2}\left(\frac{Cp_{\text{L}}}{\Delta h_{\text{LV,L}}}\right)\left(\frac{dT_{\text{bub}}}{d\tilde{X}_1}\right)\right]^{-1}$.

Kubota et al. (2001)

$$\Delta P = \Delta P_{\text{M}} + \Delta P_f,\ \Delta P_{\text{M}} = \frac{4Gqx}{d_{\text{h}}\Delta h_{\text{LV}}\rho_{\text{V}}}\left[\left(1 - \frac{1}{\varepsilon\Gamma}\right)\left(1 + \frac{1-x}{x}\varepsilon\right) + \left(1 + \frac{1-x}{x\varepsilon\Gamma}\right)\left(1-\varepsilon\right)\right] \tag{12}$$

where, $\varepsilon = \left(\frac{1-x}{x}\right)\left(\frac{\xi_{\text{smith}}}{1-\xi_{\text{smith}}}\right)\left(\frac{1}{\Gamma}\right)$ $\Gamma = \rho_{\text{L}}/\rho_{\text{V}}$ $\Delta P_{\text{F}} = \Phi_{\text{L}}^2\Delta P_{\text{F,L}}$, $\Phi_{\text{L}} = 1 + 2.09\eta X_{\text{tt}}^{-0.796}$,

$\eta = \begin{cases} 1 \text{ for annular flow} \\ 1 - \exp\left(-1.39Fr^{0.711}\right) \text{ for wavy low} \end{cases}$ $Fr = \frac{Gx}{\sqrt{\rho_{\text{V}}\left(\rho_{\text{L}} - \rho_{\text{V}}\right)d_{\text{eq}}g}}$, $f_{\text{V}} = 0.046\,\text{Re}^{-0.2}\frac{d_{\text{eq}}}{d_{\text{h}}}\sqrt{\frac{A_{\text{fa}}}{A_{\text{fn}}}}\left(\sec\beta_{\text{fin}}\right)^{0.75}$

top graph, the temperature glide and the mole fraction difference between vapor and liquid at the equilibrium state are plotted. In the middle graph, the experimental HTC and the predicted HTC are plotted using symbols and lines, respectively. Similarly, in the bottom graph, the experimental pressure drop and the predicted pressure drop are plotted. For the prediction, the following three correlations are selected. Earlier, an empirical model predicting the HTC inside

microfin tubes has been proposed by Cavallini et al. (1998) for pure and refrigerant mixtures R407C, R410B, R32/R134a, and R123/R134a. A summary of the correlation transcribed on the bases of the actual heat transfer area, is shown in Table 3. Recently, Kondou et al. (2013) has proposed a correlation to predict the HTC of R32/R1234ze(E) in a microfin tube with an outer diameter of 6 mm. Kubota et al. (2001) proposed a correlation to predict the pressure drop of a single component flowing in microfin tubes. For the calculation of mixtures, only the change in the physical properties of the mixtures was considered.

As shown in the top graph of Figure 5, the difference in mole fraction between vapor and liquid of vapor qualities 0.3, 0.5, and 0.7 are maximal at mass fractions 0.15, 0.2, and 0.21, respectively. Accordingly, the temperature glide is maximized at a mass fraction of 0.12 in R32/R1234yf and a mass fraction of 0.2 in R32/R1234ze(E). These equilibrium data show that R32/R1234ze(E) exhibits a large volatility difference in a wide range of mass fractions. R32/R1234yf exhibits a more moderate volatility difference at mass fractions above 0.7.

As shown in the middle graph of Figure 5, the HTC values of the mixtures are lower than those of the single components in most of the mass fraction range. The heat transfer of the mixture is severely degraded in the mass fraction range 0.1 to 0.6 for R32/R1234yf, and in the range 0.1 to 0.8 for R32/R1234ze(E). In these ranges, the predicted HTC agrees well with the experimentally determined HTC. The variation in HTC is inversely related to the variation in the mole fraction difference. This relation confirms the mechanism of heat transfer degradation caused by the volatility difference as stated in previous studies. Therefore, the HTC of R32/R1234yf is slightly higher than that of R32/R1234ze(E). The HTC of R32/R1234yf is nearly ideal at mass fractions above 0.7, where the volatility difference is moderate. In this regard, the R32/R1234yf is favorable, relative to R32/R1234ze(E), for keeping the heat exchanger size small. However, none of the selected correlations satisfactorily predicated this HTC behavior for R32/R1234yf.

The pressure drop with R32 is lower than that with R1234yf or R1234ze(E) because R32 has a lower viscosity and a higher vapor density. The pressure drop of the mixtures moderately decreases as the mass fraction of R32 increases. The predicted pressure drop, which considers only the property change, agrees with the experimental pressure drop. This comparison indicates that the volatility difference does not affect the momentum transfer.

4. CONCLUSIONS

The heat transfer coefficients and the pressure gradients of the binary mixtures R32/R1234yf and R32/R1234ze(E) in horizontal microfin tubes have been experimentally investigated in this study. The heat transfer is degraded most at the composition where the temperature glide and mole fraction difference between vapor and liquid phases are maximum. This result suggests that the heat transfer degradation is most dependent on the mass transfer resistance caused by the concentration boundary layer and the reduction of effective wall superheating. Although the heat transfer coefficients of R1234yf and R1234ze(E) are comparable, the magnitude of heat transfer degradation is greater for R32/R1234ze(E) than for R32/R1234yf. This can be explained by the higher volatility difference of R32/R1234ze(E) compared to R32/R1234yf. The heat transfer degradation of R32/R1234yf is mitigated considerably at R32 mass fractions above 0.7. In this regard, R32/R1234yf is favorable, relative to R32/R1234ze(E).

NOMENCLATURE

A_{fa}	actual cross sectional area	(m^2)
A_{fn}	nominal cross sectional area	(m^2)
Cp	specific heat	($J\ kg^{-1}\ K^{-1}$)
D_{12}	mutual diffusion coefficient	($m^2 s^{-1}$)
D_o	outer diameter	(m)
G	mass flux	($kg\ m^{-2} s^{-1}$)
M	molar weight	(g)
Nu	Nusselt number	(-)
P	pressure	(Pa)
P_R	reduced pressure	(-)
Q	heat transfer rate	(W)
Re	Reynolds number	(-)

T	temperature	(°C)
X	mass fraction in liquid	(kg/kg)
$\widetilde{X}$	mole fraction in liquid	(mole/mole)
$\widetilde{Y}$	mole fraction in vapor	(mole/mole)
a	thermal diffusivity	(m^2s^{-1})
d	inner diameter	(m)
f	frictional coefficfient	(-)
g	gravitational acceleration	(m s^{-2})
h	specific enthalpy	(J kg^{-1})
h_{fin}	fin height	(m)
q	heat flux	(W m^{-2})
u	velocity	(m s^{-1})
x	vapor quality	(-)
Xtt	Lockhart-Martinelli parameter	(-)
ΔT_{glide}	temperature glide	(K)
ΔZ	tube length	(m)
Δh_{LV}	latent heat of vaporization	(J kg^{-1})
α	heat transfer coefficient	(W $m^{-2}K^{-1}$)
β	helix angle	(°)
η_A	surface enlargement	(-)
λ	thermal conductivity	(W $m^{-1}K^{-1}$)
μ	viscosity	(Pa s)
ρ	density	(kgm^{-3})
σ	surface tension	(Nm^{-1})
ξ	void fraction	(-)

Subscript

1	the less volatile component
2	the more volatile component
H2O	water
L	liquid
LO	liquid only
R32	R32
V	vapor
VO	vapor only
bub	bubble point
cv	convective evaporation
dew	dew point
eq	equivalent
f	mixed fluid
h	hydraulic
id	ideal
in	inlet
max	fin root
min	at fin tip diameter
mix	mixture
nb	nucleate boiling
out	outlet
r	refrigerant
sat	saturation
tube	microfin tube
wi	inner wall
wo	outer wall

REFERENCES

Myhre, G., Shindell, D., Bréon, F.-M., Collins, W., Fuglestvedt, J., Huang, J., Koch, D., Lamarque, J.-F., Lee, D., Mendoza, B., Nakajima, T., Robock, A., Stephens, G., Takemura, T., Zhan, H., (2013). Anthropogenic and Natural Radiative Forcing, in: Climate Change 2013: The Physical Science Basis. Contribution of Working Group I to the Fifth Assessment Report of the Intergovernmental Panel on Climate Change.

ASHRAE agenda-ttachment4-2015. IMC code change proposal SSPC34 meeting 24 January 2015- Chicago, IL, draft1.

Wang, X., Amrane, K., 2014. AHRI Low Global Warming Potential Alternative Refrigerants Evaluation Program (Low-GWP AREP) – Summary of Phase I Testing Results. Int. Refrig. Air Cond. Conf. Paper1416, 10.

Wettermann, M., Steiner, D., 2000. Flow boiling heat transfer characteristics of wide-boiling mixtures. Int. J. Therm. Sci. 39, 225–235. doi:10.1016/S1290-0729(00)00241-6

Jung, D.S., Radermacher, R. (1989). Prediction of pressure drop during horizontal annular flow boiling of pure and mixed refrigerants. *Int. J. Heat Mass Transf.*, 32, 2435–2446.

Lemmon, E., McLinden, M., (2013).

Kondou, C., BaBa, D., Mishima, F., Koyama, S., 2013. Flow boiling of non-azeotropic mixture R32/R1234ze(E) in horizontal microfin tubes. *Int. J. Refrig*. 36, 2366–2378.

Diani, A., Mancin, S., Rossetto, L., 2015. Flow boiling heat transfer of R1234yf inside a 3.4mm ID microfin tube. Exp. Therm. Fluid Sci. 66, 127–136.

Stephan, P., Kern, J., 2004. Evaluation of heat and mass transfer phenomena in nucleate boiling. Int. J. Heat Fluid Flow 25, 140–148.

Thome, J.R., 1983. Prediction of binary mixture boiling heat transfer coefficients using only phase equilibrium data. Int. J. Heat Mass Transfer 26 (7), 965-974.

Celata, G.P., Cumo, M., Setaro, T., 1994. A review of pool and forced convective boiling of binary mixtures. Exp. Therm. Fluid Sci. 9, 367-381.

Stephan, K., 1992. Heat transfer in condensation and boiling. Translated by Green, C.V., Springer-Verlag, Berlin, Heidelberg, 286-291.

Kern, J., Stephan, P., 2003. Theoretical Model for Nucleate Boiling Heat and Mass Transfer of Binary Mixtures. J. Heat Transfer 125, 1106.

Cavalllini, A., DelCol, D., Longo, G.A., Rosset, L., 1998. Refrigerant vaporization inside enhanced tubes. In: Proc. Heat Transfer in Condensation and Evaporation: Eurotherm seminar, Grenoble, France, 222-231.

Kubota, A., Uchida, M., Shikazono, N., 2001. Predicting equations for evaporation pressure drop inside horizontal smooth and grooved tubes. Trans. JSRAE, 18 (4), 393-401(in Japanese).

ACKNOWLEDGEMENT

This study is sponsored by the project on the "Development of High Efficiency and Non-Freon Air Conditioning Systems" of the New Energy and Industrial Technology Development Organization (NEDO), Japan. The tested microfin tube was kindly donated by Kobelco & Materials Copper Tube CO., LTD.